ACS APPLIED MATERIALS & INTERFACES

Research Article

www.acsami.org

Chitosan Derivatives Cross-Linked with Iodinated 2,5-Dimethoxy-2,5-dihydrofuran for Non-Invasive Imaging

Paulomi Ghosh,[†] Manisit Das,[†] Arun Prabhu Rameshbabu,[†] Dipankar Das,[‡] Sayanti Datta,[†] Sagar Pal,[‡] Asit Baran Panda,[§] and Santanu Dhara*[,†]

[†]Biomaterials and Tissue Engineering Laboratory, School of Medical Science and Technology, Indian Institute of Technology Kharagpur, Kharagpur 721302, India

[‡]Polymer Chemistry Laboratory, Department of Applied Chemistry, Indian School of Mines, Dhanbad 826004, India

[§]Discipline of Inorganic Materials and Catalysis, Central Salt and Marine Chemicals Research Institute (CSIR), Bhavnagar 364002, India

Supporting Information

ABSTRACT: Radiopaque polymer derivatives were successfully prepared through surface diffusion mediated cross-linking of chitosan with iodinated 2,5-dimethoxy-2,5-dihydrofuran. The incorporation of iodine in 2,5-dimethoxy-2,5-dihydrofuran was validated by ^{1}H NMR and mass spectroscopy. The cross-linking of the glucosamine moieties of chitosan with the iodinated product was confirmed by ^{13}C NMR and energy-dispersive X-ray spectroscopy. Radiography analysis proved inherent opacity of the iodinated fibrous sheets and microspheres that were comparable to the X-ray visibility of aluminum hollow rings of equivalent thickness and commercially available radiopaque tape, respectively. Microscopic studies evidenced retention of the fiber/microsphere morphology after the iodination/cross-linking reactions. The effects of iodination/cross-linking on the mechanical and biodegradation properties of fibers were studied by nanoindentation and enzymatic assay, respectively. In vitro and in vivo studies established the nontoxic, biodegradable nature of radiopaque derivatives. Iodinated fiber mesh implanted in a rabbit model was significantly X-ray opaque compared to the uncross-linked fiber mesh and medical grade surgical swabs. Further, opacity of the iodinated mesh was evident even after 60 days, though the intensity was reduced, which indicates the biodegradable nature of the iodinated polymer. The opacity of the iodinated sutures was also established in the computed tomography images. Finally, the sufficient in vivo contrast property of the radiopaque microspheres in the gastrointestinal tract indicates its possible role in clinical diagnostics.

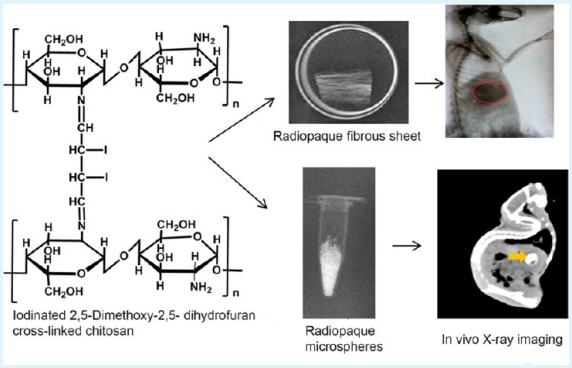

KEYWORDS: *iodination, 2,5-dimethoxy-2,5-dihydrofuran, covalent cross-linking, X-ray opacity, radiopaque sutures, gastrointestinal tract*

1. INTRODUCTION

Radiopaque materials have the ability to absorb X-rays because of their high electron density, which facilitates noninvasive post operative assessments.[1−4] In the past, radiopaque polymer blends were prepared using inorganic salts of heavy elements like $BaSO_4$ (atomic number, Z = 56 for barium), BaF_2, and $BiCl_3$ (Z = 83 for bismuth).[5−8] Of all these, mostly $BaSO_4$ was utilized for specific clinical applications such as bone cements and dental fillings.[6] However, the addition of $BaSO_4$ was found to be detrimental to the mechanical properties.[9] Further, it was reported that the release of Ba^{2+} could cause rise in the activity of osteoclasts and augment the bone resorption process; hence, researchers continue to explore alternatives wherein an X-ray opacifier is chemically bound to a biocompatible polymer.

Iodine (Z = 53) is widely used to enhance radiopacity because of its great mass attenuation and documented low systemic toxicity.[10,11] The literature reports two conceptual approaches to covalently bind iodine on polymer backbone, that is, either the introduction of iodine in the monomers before polymerization or grafting iodine on preformed high molecular weight polymers. The first conceptual approach was investigated extensively with methacrylate derivatives like methyl methacrylate (MMA) and 2-hydroxyethyl methacrylate (HEMA). Copolymerization reactions of MMA or HEMA with aromatic iodine containing vinyl monomers, namely tri-iodophenyl methacrylate, 2-hydroxy-3-methacryloyloxypropyl-(2,3,5-triiodobenzoate), 2-methacryloyloxyethyl(2,3,5-tri-iodo-benzoate) (MAOTIB), 3-acetylamino-2,4,6-triiodo benzoyl chloride, and 2-[4′-iodobenzoyloxy]-ethyl methacrylate (4-IEMA), are extensively reported for applications ranging from

Received: July 16, 2014
Accepted: September 29, 2014
Published: September 29, 2014

Table 1. Comparative Radiopacity Assessments of Chitosan Derivatives with Aluminum Samples and Commercially Available Radiopaque Tape of Equivalent Thickness

sample	DHF (mM)	iodine (mM)	time (min)	opacity (%)
ChN			5	20 ± 1.5*
CD	1150		5	22 ± 2.2
CDI_{29}	2.4	1.2	5	29 ± 4.1
CDI_{44}	38.0	19.2	5	44 ± 4.3
CDI_{58}	1150	570	5	58 ± 5.1
CDI_{85}	1150	570	10	85 ± 6.6
CDIm	1150	570	10	94.6 ± 6.5
Al	N/A	N/A	N/A	85 ± 4.3
empty tube	N/A	N/A	N/A	N/A
radiopaque tape	N/A	N/A	N/A	95.1 ± 6.8

ChN, uncross-linked fiber; CD, DHF cross-linked fiber; CDI_x, iodinated DHF cross-linked chitosan, x = average opacity; CDIm, iodinated microspheres; Al, aluminum hollow rings; empty tube, negative control; radiopaque tape, positive control; N/A, not applicable; opacity presented as mean ± SD, $n = 3$, $p < 0.05$ with respect to ∗.

denture base to bone cement and vertebroplasty.[12−20] The second conceptual approach of grafting iodine on preformed high molecular weight polymer, as in the case of cellulose acetate iodobenzoate mixed esters, was reported to be useful in embolic liquids for the treatment of cerebral aneurysms and arteriovenous malformations.[21]

Despite extensive research on methacrylate derivatives, the hydrophobicity and toxicity of MMA are well recognized.[22,23] Health care workers suffer from hypersensitivity, asthmatic reactions, local neurological symptoms, and local dermatological reactions due to prolonged exposure to MMA.[24,25] In this context, the use of nontoxic reactants will be a significant advancement in clinical applications. Chitosan, a naturally occurring biodegradable aminopolysaccharide, is structurally similar to glycosaminoglycans of extracellular matrix found in tissues and is used as tissue engineering scaffolds.[26−31] Chitosan was made X-ray opaque by mixing with iopamidol (a nonionic contrast agent) for diagnosing circulatory disorders;[32−34] however, physical mixing of the contrast agent with chitosan might result in sedimentation and leakage, which could cause toxicity to the adjacent tissues.

The present study is directed toward the development of radiopaque chitosan fibers/microspheres through cross-linking reactions. Iodine was covalently bonded to the unsaturated sites of butenedial, which was subsequently employed for cross-linking with the glucosamine moieties of chitosan. Radiopacity and the other physical properties could be modulated by varying the iodine/cross-linker molar ratio and the cross-linking time. The iodinated derivatives were further evaluated for in vitro and in vivo opacity studies.

2. EXPERIMENTAL SECTION

2.1. Fabrication of the Iodinated Derivatives. *2.1.1. Synthesis of Iodinated 2,5-Dimethoxy-2,5-dihydrofuran.* Iodine (Aldrich, M_W = 253.81 g/mol) was dissolved in 30% ethanol (Aldrich, high-performance liquid chromatography (HPLC) grade, >99.8%) and mixed with 2,5-dimethoxy-2,5-dihydrofuran (DHF) (Aldrich, M_W = 130.14 g/mol) under constant stirring at 25 °C as shown in Table 1. The undissolved solid if any was filtered off, and the iodinated residue was purified. The iodinated product (10 mg) was dissolved in 1 mL of deuterium oxide (D_2O) (Aldrich, M_W = 20.03 g/mol) and run through proton nuclear magnetic resonance (^{1}H NMR) using an Advance DAX-400 (Bruker, Sweden) 400 MHz NMR spectrometer at 30 °C. The ^{1}H NMR spectrum of the native DHF was also recorded for comparison with the iodinated product. Further, the samples were dissolved in acetonitrile (Merck, India) to obtain mass spectra using a Xevo G2 QTof (Waters, UK).

2.1.2. Cross-Linking of Chitosan with Iodinated DHF. Gelation kinetics of 6 wt % chitosan solution (MW, 710 000; > 90% deacetylated, Marine Chemicals, India) in the presence of NaOH (Merck, India) solution, DHF, and iodinated DHF were investigated as provided in the Supporting Information. On the basis of the preliminary rheological characterizations, pH-induced neutralization was employed to form uncross-linked chitosan fibers. Thereafter, the glucosamine moieties of chitosan were cross-linked with dialdehydes of DHF, pH 2.2 at 65 °C, as per our earlier report.[31] Alternatively, the uncross-linked fibers were also cross-linked with different ratios of iodinated-DHF solution for specified time periods (Table 1). Uncross-linked microspheres were prepared as provided in the Supporting Information and were also cross-linked with the iodinated DHF. The fibers/microspheres were then repeatedly washed with ethanol. Since iodine has high solubility in ethanol, unreacted iodine residue is expected to be washed out with ethanol.

2.2. Determination of Radiopacity. Radiographic images of chitosan fibrous sheets (1 mm thick) and microspheres were obtained in a digital X-ray system (AGFA CR 30-X, USA). The X-ray beam on the samples was irradiated for 0.16 ms, and the experimental parameters were 50 kV and 50 mA. X-ray images were then converted to gray scale intensity for opacification scoring using MATLAB software and compared with a commercially available 1 mm thick radiopaque tape (Komal Healthcare Pvt. Ltd., India) and aluminum hollow rings of equivalent thickness on the same radiograph. Here, it is to be noted that the iodinated DHF cross-linked chitosan fibers were named as CDIx (Table 1), where C, D, I, and x correspond to chitosan, DHF, iodine, and their opacification intensity, respectively.

2.3. Characterization of the Iodinated Derivatives. Surface features of the dried chitosan fibers and microspheres before and after the incorporation of iodine were examined using scanning electron microscopy (SEM) (EVO 60 ZEISS, Carl Zeiss SMT AG, Oberkochen, Germany) under vacuum after gold coating using a plasma sputtering unit. Samples without gold coating were used for chemical analysis using energy-dispersive X-ray spectroscopy (EDX) mapping. Solid state ^{13}C NMR spectra of the iodinated derivatives were recorded at 500 MHz on a Bruker Advance II-500NMR spectrophotometer. Nanoindentation and in vitro degradation of the chitosan fibers (n = 5) were carried out as provided in the Supporting Information.

2.4. In Vitro Assay. Cell culture was performed as provided in the Supporting Information.

2.5. In Vivo Studies. In vivo studies were performed under compliance of the Institutional Animal Ethical Committee guidelines of the Indian Institute of Technology, Kharagpur, India. New Zealand white male rabbits (~2 kg) and rats (~300 g) were housed in an atmosphere of controlled temperature and humidity. Prior to the start of the experiment, the skin of the rabbits was shaved, wiped with a 5% aqueous solution of povidone−iodine (Hixadine, Hicks Thermometers Limited), and local anesthesia (lignocanine hydrochloride, 2%, Neon)

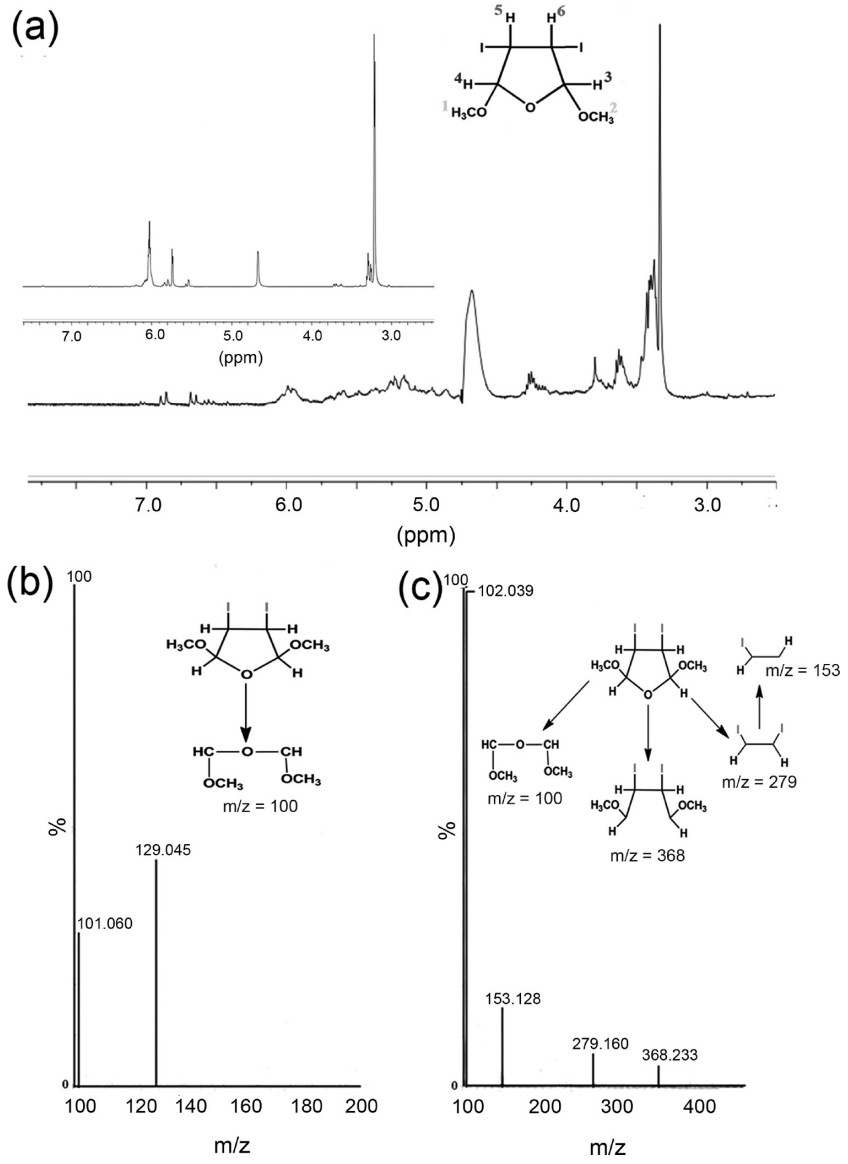

Figure 1. Synthesis of iodinated DHF. (a) ^{1}H NMR spectrum of iodinated DHF dissolved in D_2O. The inset shows the ^{1}H NMR spectrum of native DHF. MS of (b) DHF and (c) iodinated DHF.

was provided. Thereafter, an incision was made in the skin to implant unwoven chitosan fiber mesh for investigation using X-ray radiography at specified time intervals (24 h and 60 days). Medical grade surgical swabs (Johnson–Johnson, India) were used as control. Thereafter, the animals were sacrificed, and the retrieved samples were analyzed for routine histology. The sutures fabricated from radiopaque and uncross-linked fibers were subcutaneously implanted and investigated with computed tomography (CT) (Siemens somatom spirit dual-slice CT, 30 mA/s, 130 kW) imaging studies after 21 days. Catgut sutures (Johnson–Johnson, India) were used as controls.

Further, orally administered iodinated microspheres were investigated in the gastrointestinal tract (GIT) of rats using CT imaging as per an earlier report.[35] Briefly, the animals were fed with 2 mL of laxative (Isabgol, Dabur Nature Care, India) over 2 h using gavage needles and then fasted for 6 h with free access to water before the administration of the iodinated microspheres. The in vivo contrast properties of the microspheres dispersed in saline (dose 30 mg/kg) were then observed using CT imaging at 1 h and 3 h after oral administration.

2.6. Statistical Analysis. Each experiment was repeated in triplicate, and the data are presented using mean ± standard deviation (SD). Statistical analysis was performed by independent *t* test where two independent variables were used. An analysis of variance (ANOVA) was used where multiple variables were compared followed by Tukey post hoc analysis in OriginPro 8 software. Significance was determined at $p < 0.05$.

3. RESULTS

3.1. Fabrication of Iodinated Derivatives. *3.1.1. Synthesis of Iodinated DHF.* Proton NMR and mass spectroscopy (MS) provided comprehensive information regarding the electrophilic addition of iodine in the olefinic units of DHF (Figure 1). Figure 1, panel (a) displays ^{1}H NMR of iodinated DHF and native DHF (inset of Figure 1a). Three peaks at δ = 3.145–3.313(s) could be attributed to methoxy proton (H1 and H2) having cis and trans isomers, and the peaks at δ = 3.633–3.724(m) are due to H3 and H4 protons. Peaks at δ = 5.534–6.109(m) are due to H5 and H6 protons, which evidences some degree of unsaturation. This is supported by a previous study that reported lower alkene diiodide could not be prepared completely free of the olefin because of slow decomposition to iodide and alkene at room temperature.[36]

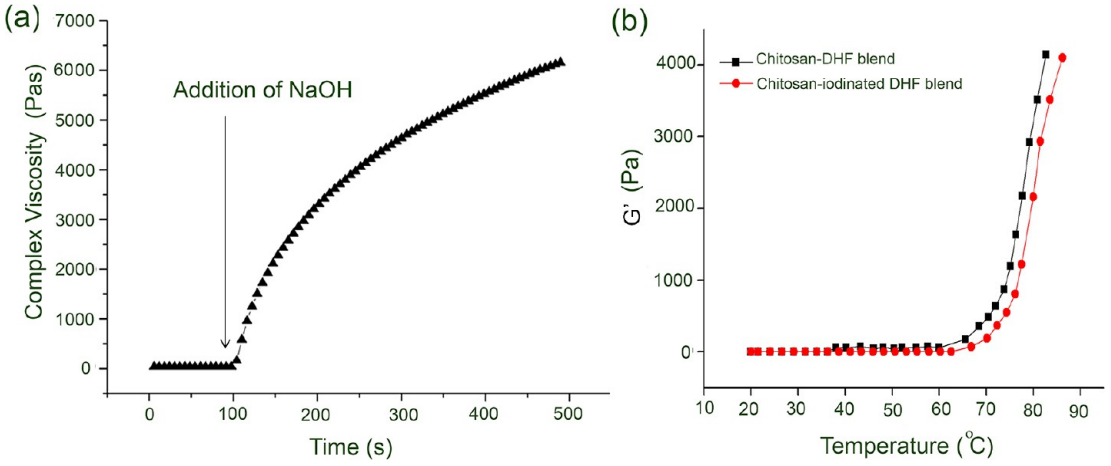

Figure 2. Rheological assessments of 6 wt % chitosan with NaOH solution, pH 13 and DHF, pH 2.2. (a) Complex viscosity of chitosan after addition of NaOH solution (5% *w*/*v*) at 25 °C as a function of time. (b) Elastic modulus (*G*′) of chitosan−DHF and chitosan−iodinated DHF blends under temperature sweep (0−90 °C) at a constant frequency and shear stress of 1 Hz and 10 Pa, respectively.

Scheme 1. Schematic Representation of Chitosan Fiber/Microsphere Formation. (a) Fabrication of Chitosan Derivatives via pH-Induced Neutralization; Chitosan Derivatives Covalently Cross-Linked with (b) DHF and (c) Iodinated DHF at pH 2.2, 65 °C

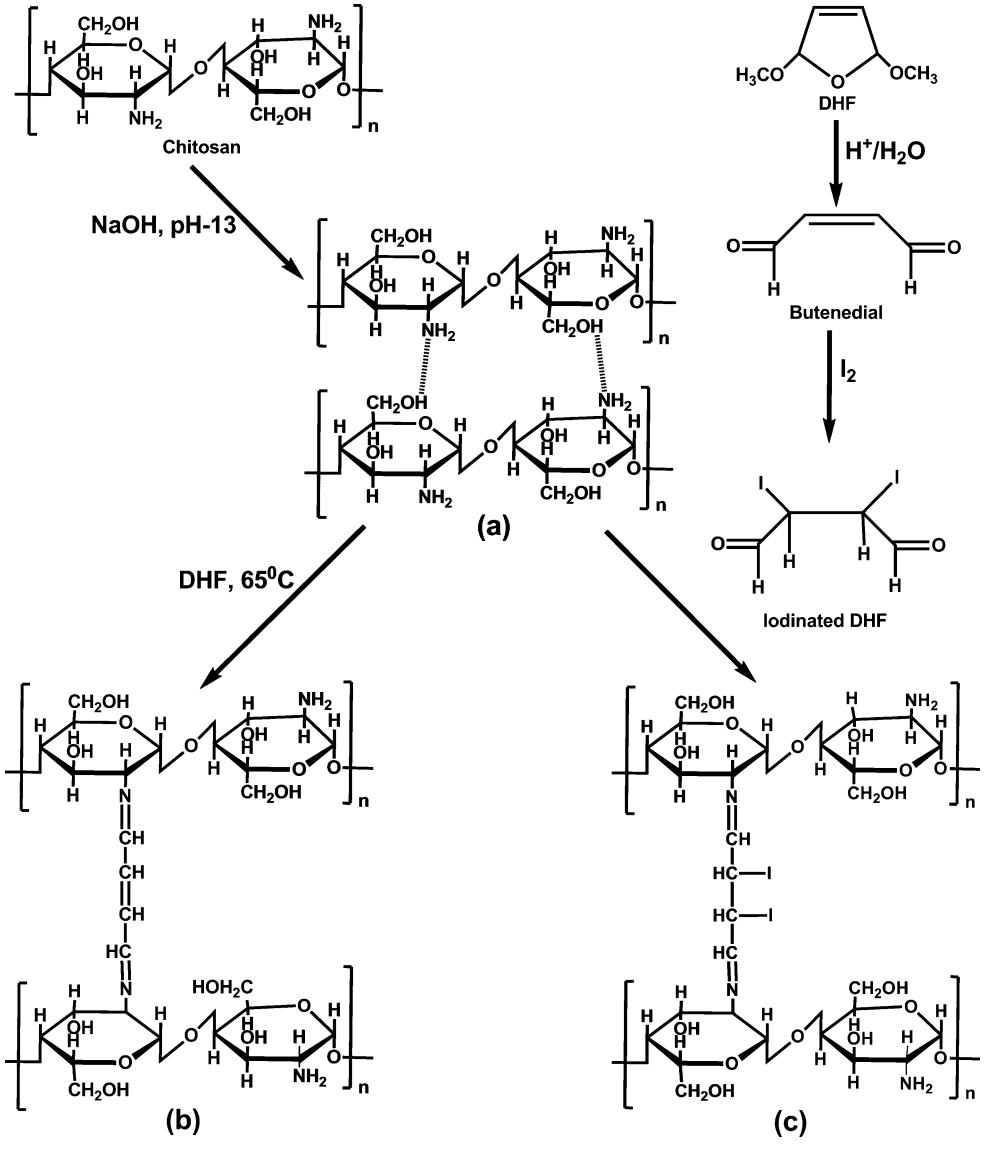

dx.doi.org/10.1021/am504655v | ACS Appl. Mater. Interfaces 2014, 6, 17926−17936

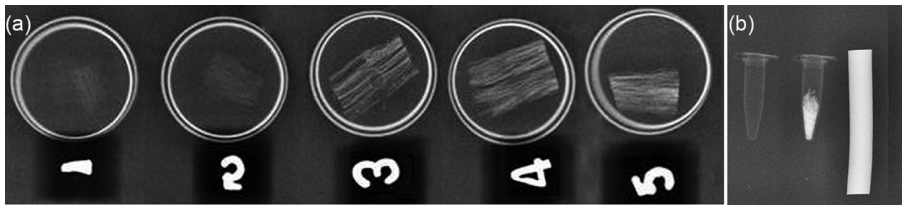

Figure 3. Radiograph showing X-ray opacity of the chitosan derivatives. (a) Fibrous sheets (average thickness of 1 mm) placed in the hollow aluminum rings of equivalent thickness (1, uncross-linked chitosan; 2, DHF cross-linked chitosan; 3, CDI_{44}; 4, CDI_{58}; 5 CDI_{85}) (3, 4, and 5 are chitosan fibrous sheets cross-linked with iodinated DHF, C = chitosan, D = DHF, and I = iodine, and the subscript = average opacity); (b) X-ray visibility of empty eppendorf, eppendorf containing radiopaque microsphere, CDIm, and commercially available radiopaque tape (from left to right).

In contrast, prominent peaks were found at 5.5−6.1 (inset of Figure 1a), which indicates the presence of unsaturation in the native DHF molecules. Thus, it is confirmed that the vinyl groups of DHF were used for iodination reactions. The peak at δ = 4.675 indicates the presence of D_2O and water mixture. Figure 1, panels b and c show MS of DHF and iodinated DHF, respectively. MS/MS spectra of DHF displays only 2 peaks—a parent peak at m/z = 129 and the fragmented sequence (H3COCHOCHCOCH3) at m/z = 100. The formation of iodinated DHF was confirmed by the increase in the molecular weight of the product. Besides the peak at m/z = 100, three new peaks were obtained. The peaks at m/z values of 153 and 279 might be fragmented parts of the parent iodinated DHF, namely, CHI-CH and CHI-CHI, respectively.

3.1.2. Cross-Linking of Chitosan with Iodinated DHF. The complex viscosity (η^*) of chitosan solution increased instantly upon the addition of NaOH solution and reached a plateau in 400 s (Figure 2a). Mechanistically, glucosamine moieties of chitosan are protonated in acetic acid, which promotes gelation of the polymer via pH-induced neutralization in alkaline solution (Scheme 1a). The instantaneous gel forming ability of chitosan in alkaline conditions was successfully used for fiber formation via the wet spinning method according to our previous work.[31] The fibers that formed were flexible in nature, white in appearance, and were named ChN. The temperature sweep measurement of chitosan−DHF and chitosan−iodinated DHF blends demonstrated a rise in the elastic modulous (G') due to progressive liquid−gel transition at elevated temperature (Figure 2b). Actually, the glucosamine units of chitosan were cross-linked with dialdehydes of DHF or iodinated DHF, at acidic pH, 65 °C, which formed a Schiff base (Scheme 1b,c). This is in agreement with previous reports;[31,36,37] however, gelation kinetics of chitosan with DHF/iodinated DHF were slow; therefore, in situ cross-linking and fiber formation were not achieved in DHF bath (data not shown). The fibers formed in NaOH bath were cross-linked in an additional step with DHF/iodinated DHF forming red and reddish brown colored fibers, respectively. Further, chitosan microspheres prepared using oil in water emulsion process and were also reacted with iodinated DHF at 65 °C, pH 2.2 for 10 min to form radiopaque microspheres. Thereafter, the iodinated fibers/microspheres were assessed for radiopacity.

3.2. Determination of Radiopacity. Radiographic examination of different chitosan based fibrous sheets is shown in Figure 3. It is evident from the radiograph that the iodinated fibers showed differential radiopacity depending on the concentration of iodine added to the reaction mixture and their reaction time (Figure 3a). The uncross-linked (ChN) and DHF cross-linked (CD) fibers did not show significant radiopacity. Table 1 shows various molar ratios of DHF−iodine solutions in the reaction mixture heated with equivalent weight of chitosan fibers. It is observed that 1.2 mM iodine was insufficient to induce opacity (data not shown on radiograph); on the other hand, an increase in the DHF/iodine ratio facilitated significant radiopacity. The average intensity of opacification increased from 29% ± 4.1 to 58% ± 5.1 when the molar concentration of iodine increased from 1.2 mM to 570 mM, respectively (Table 1). Also, the increased duration of cross-linking led to enhancement in radiopacity. For instance, the concentration of iodine was maintained at 570 mM, and when cross-linking time was increased from 5 to 10 min, the opacity value increased from 58% ± 5.1 to 85% ± 6.6, respectively (Table 1). Further increase in the cross-linking time led to the destruction of the fiber morphology (data not shown). This is mainly due to brittleness associated with the higher extent of cross-linking as reported in a previous study.[31] The X-ray visibility of the 1 mm thick CDI_{85} fibrous sheet was comparable to the aluminum hollow rings of similar thickness; also the fibers were flexible in nature. On the basis of the opacification intensity and mechanical integrity, CDI_{85} fibers were chosen for further study and compared with the uncross-linked ones. The DHF cross-linked fibers were excluded from further studies owing to the absence of radiopacity. Interestingly, the radiopaque microspheres (CDIm) formed under similar reaction conditions to those of the CDI_{85} fibers that depicted higher X-ray contrast properties (Figure 3b). This may be due to the higher degree of surface-mediated iodination/cross-linking in microspheres because of higher surface area as compared to the fibers. Moreover, X-ray opacity of CDIm was equivalent to a commercially available radiopaque tape.

3.3. Characterization of the Iodinated Derivatives. SEM of ChN, CDI_{85}, and CDIm are shown in Figure 4, panels a−c. Morphology of the iodinated fibers and microspheres was retained after the cross-linking reactions. The presence of iodine in the radiopaque chitosan derivatives was confirmed by EDX analysis as shown in Figure 4, panels d−g. Iodine was absent in the uncross-linked fibers (Figure 4d); on the other hand, CDI_{85} fibers evidenced the presence of iodine at 4 keV. Further, the radiopaque fibers were fractured to elucidate the % iodine using EDX in its core and periphery region (Figure 4e,f). Noticeably, there was a significant difference in terms of iodine content between these two regions. The core region comprises 5.0 atomic wt % against the 32.9 atomic wt % iodine in the periphery region. This indicates that iodine was incorporated in the fibers during the surface diffusion mediated cross-linking reactions. The EDX analysis of the microspheres also evidenced the presence of iodine (Figure 4g).

Figure 5 shows the solid state ^{13}C NMR of uncross-linked and iodinated chitosan derivatives. The ^{13}C NMR of uncross-

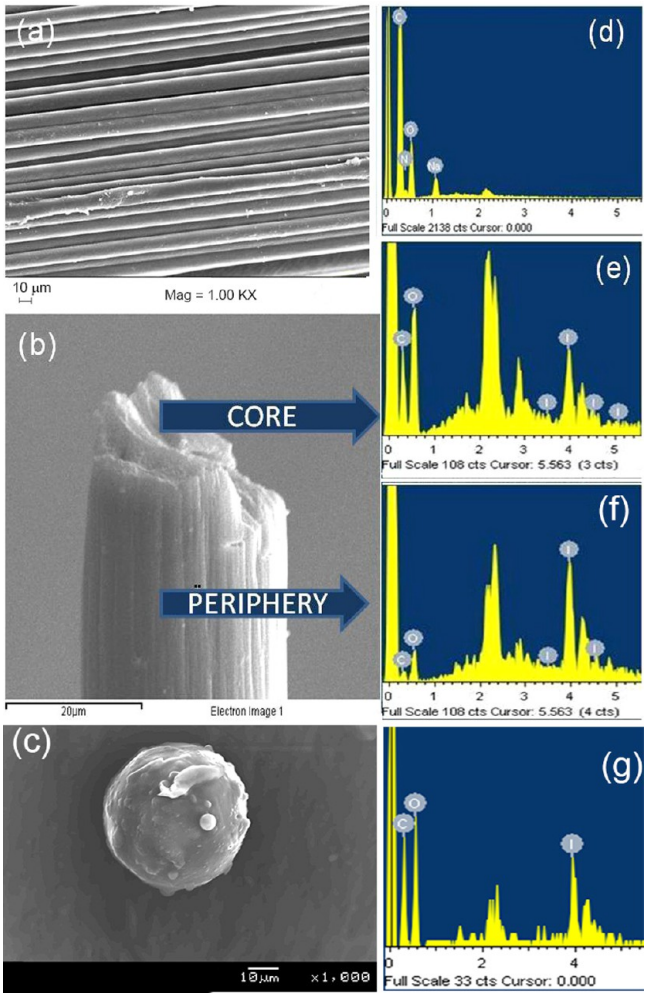

Figure 4. Characterization of chitosan derivatives. SEM images of (a) ChN, (b) CDI_{85}, and (c) CDIm; EDX of (d) ChN, fractured CDI_{85}, which shows the (e) core, (f) periphery region, and (g) CDIm. ChN, uncross-linked chitosan fibers; CDI_{85}, radiopaque fiber; and CDIm, radiopaque microsphere.

linked chitosan showed four distinct peaks in the region of 60.1−103.1 ppm, which are characteristic peaks of the carbon atoms (C1, C3, C4, C5, and C6) in the six-membered rings (Figure 5a). The peaks at 54.2 and 20.3 ppm are assigned to the carbon atom (C2) attached to the primary amine group and the methyl carbon (C8), respectively; however, a small peak at 175.2 ppm is attributed to carbonyl carbon (C7). In the case of radiopaque derivatives, because of the interaction between chitosan and the iodinated DHF, the peak values were shifted toward the higher region (Figure 5b).

The mechanical properties (average elastic modulii and hardness) improved in the iodinated chitosan derivatives because of covalent cross-linking in comparison to the uncross-linked chitosan (Supporting Information, Figure S1). This, in turn, had pronounced influence on the degradation rate of the fibers (Supporting Information). After 4 weeks of study, the enzymatic degradation rate of CDI_{85} was significantly less than that of the ChN fibers, which is mainly due to the presence of stable covalent linkages.

3.4. In Vitro Assay. The morphology of MG-63 cells cultured in media with or without iodinated DHF was evaluated on the fifth day by rhodamine−phalloidin and Dapi staining (Figure 6a,b). It is evident that the morphology of the cells cultured in media supplemented with iodinated DHF was similar to that of the cells grown in media without any additives. Further, the iodinated derivatives also supported cell attachment (Supporting Information, Figure S3). The results indicate that the iodinated DHF as well as radiopaque derivatives are cytocompatible and nontoxic in nature.

3.5. In Vivo Studies. *3.5.1. Opacity of the Fibers/Sutures.* X-ray visibility of the nonwoven fibers is depicted in Figure 7. Figure 7, panels a−c show implantation of the fiber meshes and surgical swab in the subcutaneous regions of the rabbits. The iodinated fibers were clearly discernible in X-ray after 24 h of implantation; its grade of opacity was comparable to that of the rib bones adjacent to it (Figure 7d). Notably, opacity was still evident after 60 days for CDI_{85} fiber mesh; however, the size of the mesh and intensity successively reduced as shown in Figure 7, panel e. In contrast, opacity of the control materials consisting of uncross-linked chitosan fiber mesh and medical grade surgical swabs implanted in different sides of the same

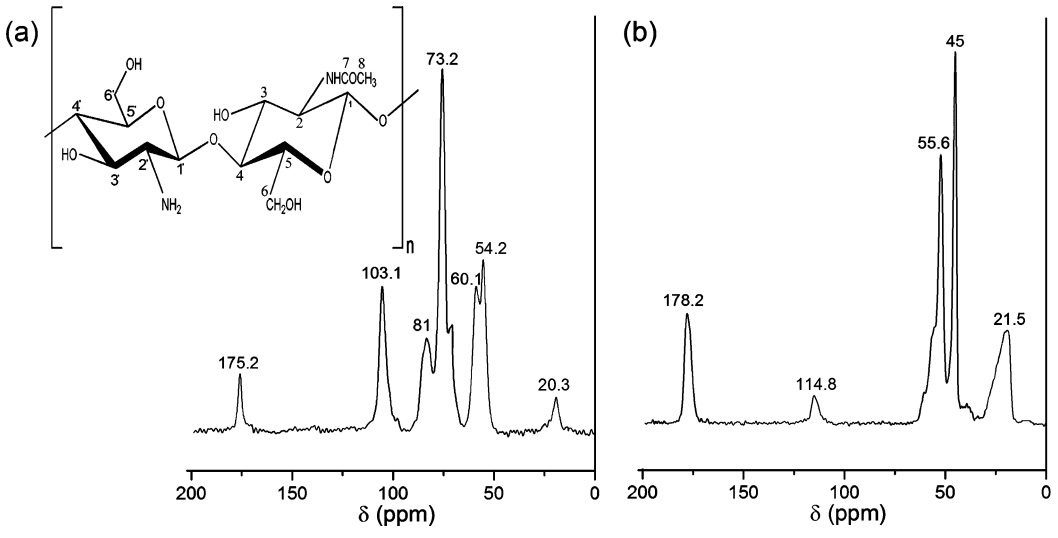

Figure 5. ^{13}C NMR spectra of (a) uncross-linked chitosan, ChN and (b) the product obtained via cross-linking of uncross-linked chitosan with iodinated DHF.

dx.doi.org/10.1021/am504655v | ACS Appl. Mater. Interfaces 2014, 6, 17926−17936

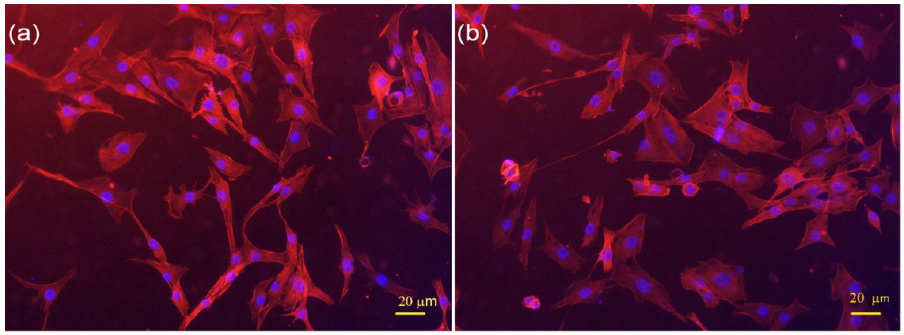

Figure 6. In vitro cytocompatibility of MG-63 cells. Representative fluorescent image of MG-63 cells on fifth day cultured in (a) Dulbecco's modified Eagle's media (DMEM) and (b) DMEM supplemented with iodinated DHF, scale bar = 20 μm.

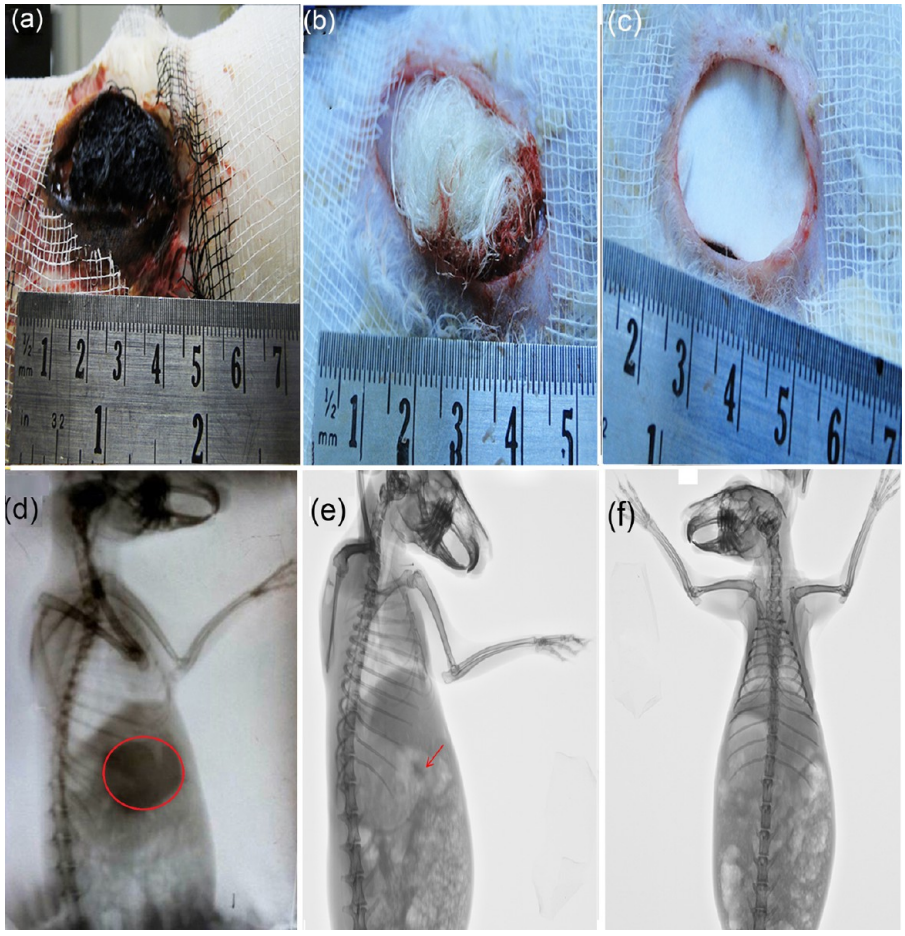

Figure 7. In vivo X-ray visibility studies of fiber mesh upon subcutaneous implantation in the rabbits. Optical image of (a) nonwoven CDI_{85}, (b) nonwoven ChN, and (c) medical grade surgical swab during implantation. ChN and the surgical swab were treated as controls and were implanted on different sides of the lower abdomen of the same rabbit. Positive X-ray print of CDI_{85} after (d) 24 h and (e) 60 days. The circle in panel d encloses the bunch of fibers after 24 h, and the arrow in panel e indicates remaining radiopaque fiber mesh after 60 days. (f) Positive print of X-ray image after 24 h for the rabbit implanted with the controls shows no radiopaque regions. ChN, uncross-linked fibers; CDI_{85}, radiopaque fibers.

rabbit was feebly visible after 24 h (Figure 7f), which indicates their radiolucent nature.

Further, the opacity of the sutures fabricated from chitosan fibers was investigated upon implantation in the lower abdomen of rabbits and compared with the catgut controls (Figure 8a,b,d,e). Radiopaque fibers retrieved after 45 days evidenced development of a thin mucous layer, which indicates tissue infiltration (Figure 8c). On the other hand, the control specimens (catgut and uncross-linked chitosan sutures) had degraded by that time period (data not shown); therefore, CT imaging studies are presented after 21 days of implantation when both the radiopaque sutures and control specimens were still distinct structurally. This is to prevent any discrepancy related to degradation issues for fair opacity comparison between the iodinated and uncross-linked chitosan sutures. CT images of the iodinated polymers (CDI_{85}) after 21 days of implantation were easily detectable with 110 Hounsfield units (HU); in comparison, the control samples were not detected in the CT image (Figure 8f). Thus, the new biomaterial displays

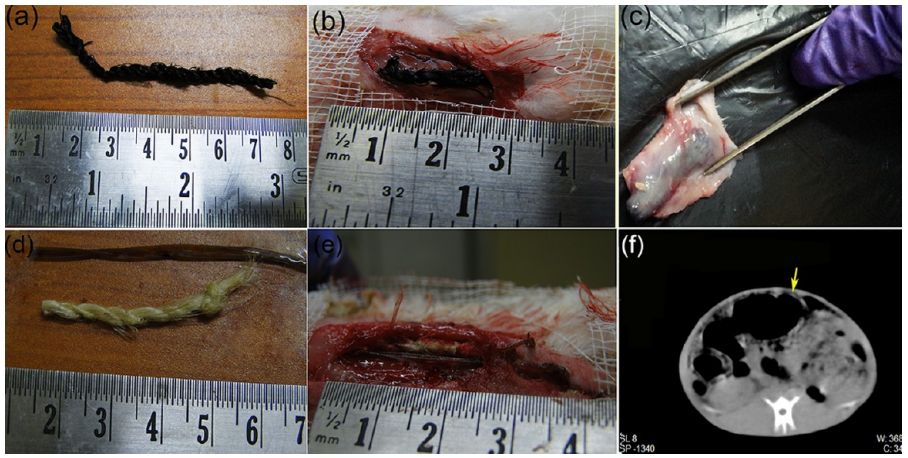

Figure 8. In vivo opacity studies of sutures upon subcutaneous implantation in rabbits. Optical images of radiopaque suture (a) before implantation, (b) during implantation, and (c) retrieval after 45 days. Optical images of uncross-linked chitosan and catgut suture treated as controls (d) before implantation and (e) during implantation. Radiopaque sutures were implanted on one side, and catgut, uncross-linked chitosan sutures were implanted on the other side of the same rabbit. (f) CT images of control specimens and radiopaque sutures after 21 days. Radiopaque suture is marked by an arrow, while on the opposite side, no appreciable opacity was detected.

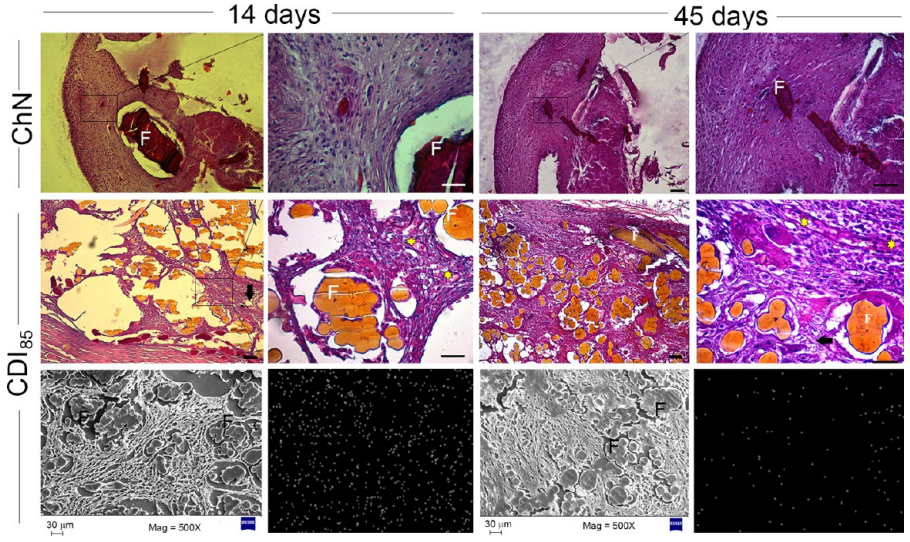

Figure 9. Representative H&E stained sections that depict in vivo host response to uncross-linked (ChN) and radiopaque chitosan fibers (CDI_{85}) implanted subcutaneously in a rabbit model (F, fibers; arrow, giant cells with multiple nuclei; star, blood vessels). Scale bar = 50 mm. Tissue sections with CDI_{85} fibers were investigated in SEM and analyzed for iodine EDX mapping (lower panel).

reasonable radiopacity, which may be visible when implanted in a large animal or human subject.

3.5.2. Histological Studies. The implanted radiopaque and uncross-linked fibers were retrieved after 14 and 45 days for histological studies (Figure 9). Hematoxylin and eosin (H&E) staining of the retrieved fibers further confirmed the degradation of the uncross-linked fibers by 45 days of implantation. In contrast, radiopaque fibers were still intact with increased cellular infiltration surrounding them. This indicates that the iodinated fibers were well integrated with the surrounding tissues. There was a notable increase in the number of infiltrated host cells after 45 days of implantation as compared to 14 days for both of the fibers. Compatibility of the subcutaneously-implanted iodinated fibers was further established by the presence of blood vessels marked with a star at 14 and 45 days. Further, the tissue sections with radiopaque fibers were investigated by SEM followed by EDX mapping for detection of traces of iodine. It was evidenced that the iodine traces were initially present in the tissue sections after 14 days but gradually decreased over time.

3.5.3. CT Imaging of the Orally Administered Iodinated Microspheres. The passage of iodinated chitosan microspheres in the GIT over time was investigated using CT imaging (Figure 10). The sagittal, coronal, and axial views at 1 h and 3 h, respectively, show opacity in the GIT, which indicates the presence of the iodinated particles. The delayed CT scan at 3 h further indicates that the microparticles were not absorbed from the GIT and could be used for GIT specific imaging purposes. The visualization of the GIT using noninvasive modalities like CT could benefit the clinical practices and research tremendously in terms of improved diagnostic accuracy of GI diseases.

4. DISCUSSION

Various strategies, including the physical mixing of heavy metals and the covalent linking of X-ray opacifiers, were devised to

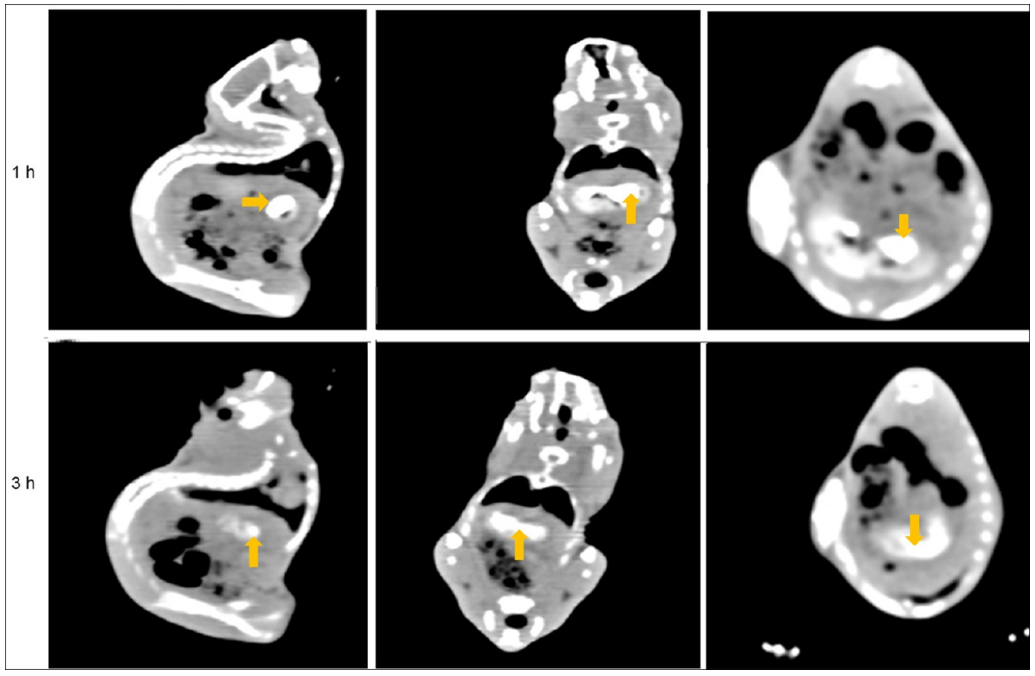

Figure 10. CT images that show the sagittal, coronal, and axial views of a rat model orally administered with iodinated microspheres after 1 h and 3 h. Yellow arrows indicate radiopaque regions.

attain the opacity of the polymers;[38,39] however, physical mixing suffers from inadequate mechanical strength and toxicity in vivo. Therefore, chemical modifications are ideal to incorporate opacity to the polymers. In the present study, we pursued iodination of the olefinic units of DHF followed by their cross-linking with glucosamine moieties of chitosan. The introduction of iodine in the unsaturated sites of DHF and subsequently to chitosan was confirmed by ^{1}H NMR, MS/MS, and ^{13}C NMR data. The differential percentage of iodine obtained by EDX mapping across the cross-section of the iodinated fibers indicated that the cross-linking reaction occurred through surface diffusion mediated Schiff base formation. Iodinated fibers exhibited graded radiopacity due to the varying degree of iodination related to the molar ratio of DHF/iodine. Interestingly, the increased time period of cross-linking also enhanced radiopacity to certain extent, after which the fiber morphology and mechanical properties were adversely affected. This may be because the longer duration of cross-linking provided iodinated DHF solution sufficient time to form extensive covalent bonds with enhanced radiopacity. The enhancement in average elastic modulus, average hardness, and decrease in degradation rate could be attributed to the covalent cross-linking of the fibers. Interestingly, the iodinated microspheres depicted enhanced X-ray opacity compared to the iodinated fibers under similar cross-linking conditions.

Rhodamine−phalloidin and Dapi staining qualitatively demonstrated regular morphology of the cells grown in media supplemented with iodinated DHF and on radiopaque fibers. Tissue integration with the radiopaque fibers, as evidenced by histocompatibility studies, revealed their suitability for clinical applications. Further, the fibers demonstrated sufficient in vivo opacity when implanted as a nonwoven fiber mesh and suture in a rabbit model by X-ray and CT imaging, respectively.

The advantage of the system is that the iodinated DHF could be used to cross-link any polymer (natural or synthetic origin), protein, or polysaccharide that has amine, unsubstituted amide, and hydroxyl moieties to prepare nontoxic radiopaque products. These novel radiopaque derivatives with tailorable biodegradability can be used in different biomedical applications like sutures, surgical swabs, and also could be woven in the form of X-ray protective aprons, gloves, or collars to protect special organs like thyroids and gonads for the safety of health care workers. In addition, the iodinated particles can be employed for the diagnosis of soft tissues like the GIT noninvasively via X-ray imaging techniques.

5. CONCLUSIONS

Iodinated chitosan fibers/microspheres were successfully fabricated via iodination and cross-linking reactions. The opacity of the radiopaque chitosan derivatives was comparable to aluminum of equivalent thickness and commercially available radiopaque tape. In vitro studies revealed nontoxicity of the iodinated products. The radiopaque fibers demonstrated improved mechanical properties in terms of elastic modulus and hardness. Tissue integration of the radiopaque fibers was demonstrated in vivo. The in vivo X-ray contrast property of the radiopaque chitosan fibers with tailorable biodegradability indicates its applicability in various biomedical and clinical fields. Furthermore, X-ray opacity of the orally administered radiopaque microspheres demonstrates its suitability for diagnostic examination of the GIT.

■ ASSOCIATED CONTENT

Supporting Information

Rheological characterization, radiopaque microsphere formation, nanoindentation, biodegradation study, and in vitro cytocompatibility. This material is available free of charge via the Internet at http://pubs.acs.org.

AUTHOR INFORMATION

Corresponding Author

*E-mail: sdhara@smst.iitkgp.ernet.in. Fax: +91-3222-282221.

Notes

The authors declare no competing financial interest.

ACKNOWLEDGMENTS

Fellowship from the Council of Scientific and Industrial Research (CSIR) to P.G. and A.P.R. is acknowledged. We are immensely grateful to Nantu Dogra and Kaushik Basak for their technical assistance. Financial aid from the Department of Biotechnology (DBT), Department of Science and Technology (DST), and CSIR, Government of India, New Delhi is acknowledged.

REFERENCES

(1) Benzina, A.; Kruft, M. A.; Bär, F.; van der Veen, F. H.; Bastiaansen, C. W.; Heijnen, V.; Reutelingsperger, C.; Koole, L. H. Studies on a New Radiopaque Polymeric Biomaterial. *Biomaterials* **1994**, *15*, 1122−1128.

(2) Chen, H.; Rogalskia, M. M.; Anker, J. N. Advances in Functional X-ray Imaging Techniques and Contrast Agents. *Phys. Chem. Chem. Phys.* **2012**, *14*, 13469−13486.

(3) Cortecchia, E.; Pacilli, A.; Pasquinelli, G.; Scandola, M. Biocompatible Two-Layer Tantalum/Titania−Polymer Hybrid Coating. *Biomacromolecules* **2010**, *11*, 2446−2453.

(4) Mazzocchetti, L.; Cortecchia, E.; Scandola, M. Organic−Inorganic Hybrids as Transparent Coatings for UV and X-ray Shielding. *ACS Appl. Mater. Interfaces* **2009**, *1*, 726−734.

(5) Wang, Q.; Zhang, D.; Yang, X.; Xu, H.; Shen, A. Q.; Yang, Y. Atom-Economical in Situ Synthesis of $BaSO_4$ as Imaging Contrast Agents within Poly(*N*-isopropylacrylamide) Microgels Using One-Step Droplet Microfluidics. *Green Chem.* **2013**, *15*, 2222−2229.

(6) Makita, M.; Yamakado, K.; Nakatsuka, A.; Takaki, H.; Inaba, T.; Oshima, F.; Katayama, H.; Takeda, K. Effects of Barium Concentration on the Radiopacity and Biomechanics of Bone Cement: Experimental Study. *Radiat. Med.* **2008**, *26*, 533−538.

(7) Romero-Ibarra, I. C.; Bonilla-Blancas, E.; Sánchez-Solís, A.; Manero, O. Influence of the Morphology of Barium Sulfate Nanofibers and Nanospheres on the Physical Properties of Polyurethane Nanocomposites. *Eur. Polym. J.* **2012**, *48*, 670−676.

(8) Davy, K. W.; Anseau, M. R.; Berry, C. Iodinated Methacrylate Copolymers as X-ray Opaque Denture Base Acrylics. *J. Dent.* **1997**, *25*, 499−505.

(9) Ingham, E.; Green, T. R.; Stone, M. H.; Kowalski, R.; Watkins, N.; Fisher, J. Production of TNF-Alpha and Bone Resorbing Activity by Macrophages in Response to Different Types of Bone Cement Particles. *Biomaterials* **2000**, *10*, 1005−1013.

(10) Dawson, P. Chemotoxicity of Contrast Media and Clinical Adverse Effects: A Review. *Invest. Radiol.* **1985**, *20*, 84−91.

(11) Mawad, D.; Poole-Warren, L. A.; Martens, P.; Koole, L. H.; Slots, T. L.; J. van Hooy-Corstjens, C. S. Synthesis and Characterization of Radiopaque Iodine-Containing Degradable PVA Hydrogels. *Biomacromolecules* **2008**, *9*, 263−268.

(12) Davy, K. W. M.; Anseau, M. R. X-ray Opaque Methacrylate Polymers for Biomedical Applications. *Polym. Int.* **1996**, *15*, 686−687.

(13) Aldenhof, Y. B.; Kruft, M. A.; Pijpers, A. P.; van der Veen, F. H.; Bulstra, S. K.; Kuijer, R.; Koole, L. H. Stability of Radiopaque Iodine-Containing Biomaterials. *Biomaterials* **2002**, *23*, 881−886.

(14) Galperin, A.; Margel, S. Synthesis and Characterization of New Micrometer-Sized Radiopaque Polymeric Particles of Narrow Size Distribution by a Single-Step Swelling of Uniform Polystyrene Template Microspheres for X-ray Imaging Applications. *Biomacromolecules* **2006**, *7*, 2650−2660.

(15) Galperin, A.; Margel, D.; Baniel, J.; Dank, G.; Biton, H.; Margel, S. Radiopaque Iodinated Polymeric Nanoparticles for X-ray Imaging Applications. *Biomaterials* **2007**, *28*, 4461−4468.

(16) Jayakrishnan, A.; Thanoo, B. C.; Rathinam, K.; Mohanty, M. Preparation and Evaluation of Radiopaque Hydrogel Microspheres Based on PHEMA/Iothalamic Acid and PHEMA/Iopanoic Acid as Particulate Emboli. *J. Biomed. Mater. Res.* **1990**, *24*, 993−1004.

(17) Wang, J. S.; Diaz, J.; Sabokbar, A.; Athanasou, N.; Kjellson, F.; Tanner, K. E.; McCarthy, I. D.; Lidgren, L. In Vitro and in Vivo Biological Responses to a Novel Radiopacifying Agent for Bone Cement. *J. R. Soc., Interface* **2005**, *2*, 71−78.

(18) Zaharia, C.; Zecheru, T.; Moreau, M. F.; Pascaretti-Grizon, F.; Mabilleau, G.; Marculescu, B.; Filmon, R.; Cincu, C.; Staikos, G.; Chappard, D. Chemical Structure of Methyl Methacrylate-2-[2′,3′,5′-triiodobenzoyl]oxoethyl Methacrylate Copolymer, Radio-Opacity, in Vitro and in Vivo Biocompatibility. *Acta Biomater.* **2008**, *4*, 1762−1769.

(19) Pepiol, A.; Teixidor, F.; Saralidze, K.; van der Marel, C.; Willems, P.; Voss, L.; Knetsch, M. L.; Vinas, C.; Koole, L. H. A Highly Radiopaque Vertebroplasty Cement Using Tetraiodinated *o*-Carborane Additive. *Biomaterials* **2011**, *32*, 6389−6398.

(20) Van Hooy-Corstjens, C. S.; Saralidze, K.; Knetsch, M. L.; Emans, P. J.; de Haan, M. W.; Magusin, P. C.; Mezari, B.; Koole, L. H. New Intrinsically Radiopaque Hydrophilic Microspheres for Embolization: Synthesis and Characterization. *Biomacromolecules* **2008**, *9*, 84−90.

(21) Mottu, F.; Rüfenacht, D. A.; Laurent, A.; Doelker, E. Iodine-Containing Cellulose Mixed Esters as Radiopaque Polymers for Direct Embolization of Cerebral Aneurysms and Arteriovenous Malformations. *Biomaterials* **2002**, *23*, 121−131.

(22) Patel, S.; Thakar, R. G.; Wong, J.; McLeod, S. D.; Li, S. Control of Cell Adhesion on Poly(methyl methacrylate). *Biomaterials* **2006**, *27*, 2890−2897.

(23) Young, J. A. Methyl Methacrylate. *J. Chem. Educ.* **2006**, *83*, 695.

(24) Leggat, P. A.; Smith, D. R.; Kedjarune, U. Surgical Applications of Methyl Methacrylate: A Review of Toxicity. *Arch. Environ. Occup. Health* **2009**, *64*, 207−212.

(25) Leggat, P. A.; Kedjarune, U. Toxicity of Methyl Methacrylate in Dentistry. *Int. Dent. J.* **2003**, *53*, 126−131.

(26) Dash, M.; Chiellini, F.; Ottenbrite, R. M.; Chiellini, E. Chitosan—A Versatile Semi-Synthetic Polymer in Biomedical Applications. *Prog. Polym. Sci.* **2011**, *36*, 981−1014.

(27) Jiang, H.; Zuo, Y.; Zou, Q.; Wang, H.; Du, J.; Li, Y.; Yang, X. Biomimetic Spiral−Cylindrical Scaffold Based on Hybrid Chitosan/Cellulose/Nano-Hydroxyapatite Membrane for Bone Regeneration. *ACS Appl. Mater. Interfaces* **2013**, *5*, 12036−12044.

(28) Sarkar, S. D.; Farrugia, B. L.; Dargaville, T. R.; Dhara, S. Physico-Chemical/Biological Properties of Tripolyphosphate Cross-Linked Chitosan Based Nanofibers. *Mater. Sci. Eng., C* **2013**, *33*, 1446−1454.

(29) Datta, P.; Ghosh, P.; Ghosh, K.; Maity, P.; Samanta, S. K.; Ghosh, S. K.; Mohapatra, P. K.; Chatterjee, J.; Dhara, S. In Vitro ALP and Osteocalcin Gene Expression Analysis and in Vivo Biocompatibility of *N*-methylene Phosphonic Chitosan Nanofibers for Bone Regeneration. *J. Biomed. Nanotechnol.* **2013**, *9*, 870−879.

(30) Ghosh, P.; Rameshbabu, A. P.; Dhara, S. Citrate Cross-Linked Gels with Strain Reversibility and Viscoelastic Behavior Accelerates Healing of Osteochondral Defects in Rabbit Model. *Langmuir* **2014**, *30*, 8442−8451.

(31) Ghosh, P.; Rameshbabu, A. P.; Dogra, N.; Dhara, S. 2,5-Dimethoxy-2,5 dihydrofuran Cross-Linked Chitosan Fibers Enhance Bone Regeneration in Rabbit Femur Defects. *RSC Adv.* **2014**, *4*, 19516−19524.

(32) Fatimi, A.; Chabrot, P.; Berrahmoune, S.; Coutu, J. M.; Soulez, G.; Lerouge, S. A New Injectable Radiopaque Chitosan-Based Sclerosing Embolizing Hydrogel for Endovascular Therapies. *Acta Biomater.* **2012**, *8*, 2712−2721.

(33) Gertz, E. W.; Wisneski, J. A.; Chiu, D.; Akin, J. R.; Hu, C. Clinical Superiority of a New Nonionic Contrast Agent (Iopamidol) for Cardiac Angiography. *J. Am. Coll. Cardiol.* **1985**, *5*, 250−258.

(34) Ahn, S.; Jung, S. Y.; Lee, J. P.; Lee, S. J. Properties of Iopamidol-Incorporated Poly(vinyl alcohol) Microparticle as an X-ray Imaging Flow Tracer. *J. Phys. Chem. B* **2011**, *115*, 889−901.
(35) Nakamura, M.; Awaad, A.; Hayashi, K.; Ochiai, K.; Ishimura, K. Thiol-Organosilica Particles Internally Functionalized with Propidium Iodide as a Multicolor Fluorescence and X-ray Computed Tomography Probe and Application for Non-Invasive Functional Gastrointestinal Tract Imaging. *Chem. Mater.* **2012**, *24*, 3772−3779.
(36) Sumrell, G.; Wyman, B. M.; Howell, R. G.; Harvey, M. C. Reaction of Lower Olefins and Iodine in a Liquid Phase: Novel Preparation of Alkene Iodohydrins. *Can. J. Chem.* **1964**, *42*, 2710−2712.
(37) Johnson, S. B.; Dunstan, D. E.; Franks, G. V. A Novel Thermally-Activated Crosslinking Agent for Chitosan in Aqueous Solution: A Rheological Investigation. *Colloid Polym. Sci.* **2004**, *282*, 602−612.
(38) Johnson, S. B.; Dunstan, D. E.; Franks, G. V. Rheology of Cross-Linked Chitosan−Alumina Suspensions Used for a New Gelcasting Process. *J. Am. Ceram. Soc.* **2002**, *85*, 1699−1705.
(39) Yin, Q.; Yap, F. Y.; Yin, L.; Ma, L.; Zhou, Q.; Dobrucki, L. W.; Fan, T. M.; Gaba, R. C.; Cheng, J. Poly(iohexol) Nanoparticles as Contrast Agents for in Vivo X-ray Computed Tomography Imaging. *J. Am. Chem. Soc.* **2013**, *135*, 13620−13623.